Kinetics of Formation of Molybdenum Selenides from Modulated Reactants and Structure of the New Compound Mo_3Se

Robert Schneidmiller, Marc D. Hornbostel, and David C. Johnson*

Department of Chemistry and Materials Science Institute, University of Oregon, Eugene, Oregon 97403

Received July 21, 1997[⊗]

The kinetics of compound formation in the molybdenum−selenium system has been investigated using elementally modulated reactants to control overall composition and diffusion length. We observed the facile formation of $MoSe_2$ at low temperatures when the composition was above 50 atom % selenium. No evidence was found for the low-temperature formation of the other known stable molybdenum selenide, the cluster compound Mo_6Se_8. When the composition of the initially modulated reactant was close to 25% selenium, a previously unreported compound was observed to form. This new compound, Mo_3Se, has the A-15 crystal structure. The superconducting transition temperature appears to be very sensitive to composition, with a sharp resistive transition at 7 K in one sample and a sharp diamagnetic transition observed in a second sample at 2.2 K. The kinetics of phase formation in this system is analyzed in terms of nucleation kinetics.

Introduction

Within the field of solid state chemistry, the synthesis of a novel compound has been described as being as much an art as a science.[1] This is because there is no general systematic method to design a synthesis for a targeted extended inorganic compound. Instead, successful synthesis depends upon the intuition of individual researchers which has been developed on the basis of closely related classes of compounds. The lack of rational synthesis methods is easily understood if one considers the synthesis of a solid that peritectically decomposes at a temperature which is low relative to that required for solid state diffusion. A survey of such a system, typically done by annealing samples at steadily decreasing temperatures, would miss this compound because the equilibration time becomes impractically long as the temperature is reduced. Since little is known about the mechanisms of conversion between solid state compounds, there is little hope for rationally decreasing this equilibration time at low temperatures.

This reflects a well-known limitation of traditional solid state reactions in which the direct reaction between solid reactants is dominated by slow diffusion rates. The traditional methods of increasing reaction rates have been to (1) raise the reaction temperature, (2) reduce the activation energy for diffusion by going to a fluid phase (melting the sample, using a solvent or flux), or (3) reduce the diffusion distances by intimately mixing the elements using either a molecular or solid state precursor.[2] Little is known about the reaction mechanisms of any of these choices. The first method is not useful in finding a compound that only exists at low temperatures. If a reaction temperature is chosen just below the peritectic decomposition temperature, there will be a slow conversion of the solid state reactants to the desired products. This is a result of the small free energy change between compounds formed as reaction intermediates and the desired final product, leading to a small driving force for conversion. The second method has produced many new compounds at relatively low temperatures; however, they are complex reacting systems and little is known regarding the species in solution in the common solvents (for example, supercritical water) or fluxes (molten salts, metals and eutectic mixtures) used in these reactions. It is therefore difficult to predict how reactions will proceed and what products might be formed. The third method overcomes some of the diffusion difficulties; however, elimination of ligands and solvents of crystallization from the macroscopic precursor particles is still a long-range diffusion problem requiring elevated temperatures and extended reaction times. In addition, design of the precursor for each new system to be investigated can, in itself, be a difficult synthetic procedure.

These complications have led us to develop the use of modulated elemental superlattices as initial reactants for the synthesis of extended inorganic solids. In these modulated elemental reactants, the diffusion distance is determined by the modulation length and is a new experimental variable that can be used to control the reaction rate and mechanism. We have shown that if the modulation length is above a critical thickness, interfacial nucleation of a crystalline compound occurs as the temperature is increased. If the modulation length is below this critical thickness, an amorphous reaction intermediate is formed as the temperature is increased. Essentially, the layers interdiffuse, eliminating the internal interfaces before the system has a chance to interfacially nucleate.[3] This amorphous intermediate is kinetically stable, and we have shown that the formation of crystalline compounds is nucleation limited.[4] The crystalline compound which forms is the easiest compound to nucleate, not necessarily the thermodynamically most stable compound.[5] The composition of the amorphous intermediate can be used to control the relative nucleation energy of crystalline compounds.[6] This synthesis approach provides control of the reaction intermediates, avoiding thermodynamic traps, such as the formation of undesired crystalline compounds.[7] While modulated reactants have overcome the diffusion problem in solid state reactions, understanding the kinetics of the new rate-limiting step, nucleation, is a considerable challenge. This understanding is crucial for the development of the ability to

[⊗] Abstract published in *Advance ACS Abstracts,* November 15, 1997.

(1) DiSalvo, F. J. *Science* **1990**, *247*, 649−655.
(2) Corbett, J. D. In *Solid State Chemistry Techniques*; Cheetham, A. K., Day, P., Eds.; Clarendon Press: Oxford, U.K., 1987; pp 1−38.
(3) Fister, L.; Johnson, D. C. *J. Am. Chem. Soc.* **1992**, *114*, 4639−4644.
(4) Fukuto, M.; Hornbostel, M. D.; Johnson, D. C. *J. Am. Chem. Soc.* **1994**, *116*, 9136−9140.
(5) Novet, T.; Johnson, D. C. *J. Am. Chem. Soc.* **1991**, *113*, 3398−3403.
(6) Oyelaran, O.; Novet, T.; Johnson, C. D.; Johnson, D. C. *J. Am. Chem. Soc.* **1996**, *118*, 2422−2426.
(7) Hornbostel, M. D.; Hyer, E. J.; Thiel, J.; Johnson, D. C. *J. Am. Chem. Soc.* **1997**, *119*, 2665−2668.

S0020-1669(97)00812-4 CCC: $14.00

fully control the solid state reaction as well as the morphology of the resulting crystalline material.

In order to control nucleation from amorphous intermediates, it is necessary to consider the nucleation barriers for the formation of different crystalline structures as a function of composition. Nucleation is the start of growth of a new phase. Conceptually, it begins with the formation of a small region of a new, stable phase within an existing unstable material. The decrease in free energy per unit volume of this small region will tend to stabilize this new phase. However, this new region is bounded by a surface that has a positive free energy per unit area which destabilizes the small region. Since nuclei are small, the ratio of surface to volume is high, and for sufficiently small regions, the surface energy will dominate the volume energy, leading to the small region reconverting to the existing unstable material. The small region must be above some critical size before the volume term dominates, leading to spontaneous growth of the stable compound.[8] In real samples, the situation is of course much more complex. Composition of the amorphous intermediate affects the free energy change per unit volume differently for each crystalline structure. Volume changes during the transformation will result in long- and short-range stress fields, which will increase the surface energy term. Impurities, grain boundaries, and inclusions often reduce the magnitude of the surface energy term. Nucleation may involve (a) the assembly of the proper kinds of atoms by diffusive motion, (b) structural changes into one or more intermediate structures, and (c) formation of nuclei of the new phase. In this work, we attempt to experimentally determine the factors that control nucleation from the amorphous intermediate, with the goal of developing a rational strategy for the synthesis of a desired structure.

We focused our attention on the binary molybdenum−selenium system because of our longstanding interest in preparing compounds that contain discrete clusters in the solid state. The ternary molybdenum chalcogenides are the best example of this type of compound in the literature.[9] Previous work has shown that the critical thickness for forming amorphous intermediates with compositions near 33% molybdenum and 67% selenium is approximately 25 Å, so we were reasonably confident that we could produce amorphous intermediates.[3] Our goal was to nucleate the known binary molybdenum selenides selectively, using composition to change the relative nucleation energies of the various products. The accepted molybdenum−selenium phase diagram is simple, containing only two known compounds. These are the layered compound $MoSe_2$ and the cluster compound Mo_6Se_8. Both of these compounds decompose peritectically: $MoSe_2$ at approximately 1150 °C to Mo_6Se_8 and selenium vapor; Mo_6Se_8 at approximately 1400 °C to molybdenum metal and selenium vapor.[10] In addition to these thermodynamically stable compounds, several metastable binary cluster compounds have been made by preparing thermodynamically stable ternary compounds and chemically removing the ternary cation at low temperatures.[11] In this study, we found that only two compounds nucleated from elementally modulated reactants prepared with a wide composition range, $MoSe_2$ and a new compound, Mo_3Se, which is stable below 550 °C.

(8) Brophy, J. H.; Rose, R. M.; Wulff, J. *The Structure and Properties of Materials*; Wiley: New York, 1964; Vol. 2, pp 98−108.
(9) Yvon, K. *Curr. Top. Mater. Sci.* **1979**, *3*, 1−53.
(10) *Binary Alloy Phase Diagrams*, 2nd ed.; Massalski, T. B., Okamoto, H., Subramanian, P. R., Kacprzak, L., Eds.; ASM International: Materials Park, OH, 1990; Vol. 3, pp 2664−2665.
(11) Chevrel, R.; Sergent, M. In *Superconductivity in Ternary Compounds. I. Structural, Electronic and Lattice Properties*; Fischer, O., Maple, M. B., Eds.; Springer-Verlag: New York, 1982; Vol. 32, pp 26−83.

Experimental Section

Sample Preparation. A custom-built deposition system with independently controlled deposition sources was used to prepare the multilayer samples.[12] Molybdenum was deposited using a Thermionics electron beam gun source, and selenium was deposited using a Knudsen cell. The deposition rate for molybdenum was actively controlled by a Leybold-Inficon XTC quartz crystal thickness monitor. The deposition rate of selenium was set by the temperature of the Knudsen cell to be near 0.5 Å/s and monitored by a crystal monitor. The background pressure was kept below 5×10^{-6} Torr during deposition. Multilayer films were simultaneously deposited on two adjacent substrates, one polished (±3 Å rms) silicon wafer (or off-cut quartz zero-background plate) and one poly(methyl methacrylate) (PMMA) coated wafer. The samples deposited on the polished wafers were used for low-angle X-ray diffraction measurements. The films on the PMMA-coated wafers were removed from the substrates by immersing the wafers in acetone. The suspended sample was filtered off, washed to remove dissolved PMMA, and then dried on the Teflon filters.

Compositional Analysis. Electron probe microanalysis (EPMA) was used to determine the composition of all as-deposited samples. Portions of the sample collected on the Teflon filters (approximately 9 mm^2) were adhered to a glass substrate by double-sided conductive carbon tape. The microprobe data were collected on a Cameca SX-50 using a 10 keV accelerating voltage, a 10 nA beam current, and a 10 μm spot size.

X-ray Diffraction. Diffraction data were collected using copper Kα radiation on a Scintag XDS-2000 $\theta-\theta$ diffractometer with a sample stage modified to allow rapid and precise alignment for low-angle measurements.[13] The low-angle diffraction pattern resulting from the periodic layered structure of the as-deposited sample was used to determine modulation thicknesses and widths of the composition profiles between elemental layers. High-angle diffraction data were used to identify crystalline elements or compounds in the as-deposited and free-standing samples as a function of annealing temperature and time. A quartz zero-background plate was used as a sample support for all high-angle work.

Differential Scanning Calorimetry (DSC). The heat evolution of the samples as they were subjected to elevated temperatures was monitored using a TA Instruments TA9000 calorimeter fitted with a 910 DSC cell. Approximately 1 mg of sample was placed into an aluminum pan and sealed by crimping for each experiment. The sample was heated from ambient temperature to 550 °C at a rate of 10 °C/min under flowing nitrogen and then allowed to cool back to room temperature. Without disturbing the sample or instrument, this cycle was repeated to measure reversible transitions in the sample as well as the cell background. The net heat flow associated with the irreversible changes occurring in the sample during the initial heating cycle were determined by subtracting the data collected during the second cycle from those for the first.

Magnetic Susceptibility. The temperature dependence of the magnetic susceptibility was collected with a Quantum Design SQUID magnetometer with an applied magnetic field of 20 G. Approximately 1 mg of free-standing sample was placed into one side of a gel cap. The "cap" end was inverted to compress the powder to discourage any "bouncing" during the measurement. The sample was cooled to 2 K with liquid helium and then heated at constant rate to 70 K.

Electrical Conductivity. The temperature dependence of the electrical conductivity was collected using a standard four-probe technique. Sample films were deposited on silicon wafer substrates and annealed for 25 min at 250 °C in a nitrogen atmosphere with less than 1 ppm of oxygen. Silver paint was used to adhere the contacts to the sample film. The sample was cooled to 2 K with liquid helium and the sample temperature controlled with an Oxford Instruments temperature controller. A sequence of increasing constant currents was passed through the current leads while the voltage drop across the voltage leads was measured. Resistance was calculated from the slope

(12) Fister, L.; Li, X. M.; Novet, T.; McConnell, J.; Johnson, D. C. *J. Vac. Sci. Technol., A* **1993**, *11*, 3014−3019.
(13) Novet, T.; McConnell, J. M.; Johnson, D. C. *Chem. Mater.* **1992**, *4*, 473−478.

Table 1. Summary of Molybdenum−Selenium Reactants Used To Explore the Low-Temperature Formation of Binary Compounds[a]

sample	intended Mo thickness, Å	intended Se thickness, Å	repeat thickness, Å	composition % Mo
A-1	6	20	26.04	30
A-2	6	17	23.2	35
A-3	6	20	27.06	35
A-4	9	21	29.14	38
A-5	4.3	9	13.4	41
A-6	4.6	9	13.7	45
A-7	4.8	9	14.07	46
A-8	6	12	20.25	47
A-9	7	9	15.3	51
A-10	6	9	15.21	53
B-1	8	9	16.08	57
B-2	10	9	18.12	63
C-1	6	5.4	11.1	66
C-2	6	4.2	8.4	69
C-3	6	3.6	10.5	70
C-4	6	4.2	10	71
C-5	6	3	9.8	74
C-6	10	5	14.63	74
C-7	7	4	10.37	74
C-8	5	2.4	7.6	76
C-9	6	3	8.91	77
D-1	23	6	28.5	86
D-2	37	5	44.0	89

[a] The repeat thickness was determined using low-angle X-ray diffraction. Compositions were determined from electron microprobe analysis.

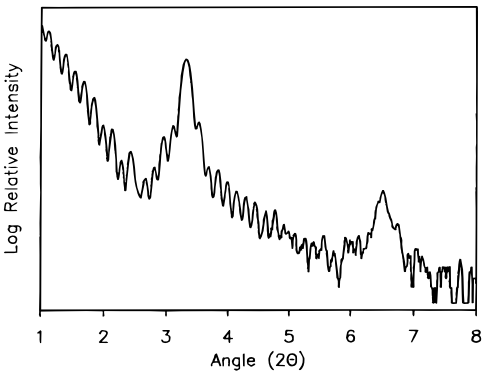

Figure 1. Representative low-angle diffraction data from an as-deposited sample (A-3). The large maxima at 3.3 and 6.6° are the first- and second-order Bragg diffraction maxima from the repeating unit of the elementally modulated sample. The smaller maxima between these peaks result from interference of the X-rays from the front and back of the deposited film.

of the *IV* curve. Resistivity was calculated from the resistance measurements using the known dimensions of the sample.

Results and Discussion

Table 1 contains a list of the samples made as part of this investigation. The goal was to prepare a number of samples of varying composition across the phase diagram. The structure of the as-deposited samples were probed using low-angle X-ray diffraction. An example of a low-angle diffraction scan is shown in Figure 1. The repeat thickness was determined from the position of the Bragg diffraction maxima. The total film thickness was determined from the higher frequency oscillations resulting from interference from the front and back of the films. The repeat thicknesses were, except for those of very selenium- or molybdenum-rich samples, kept below 25 Å, because a previous study determined that the critical thickness for compositions near 66% selenium was approximately 25 Å.[3] The agreement between the intended and actual repeat thicknesses for the samples in this table is generally within 2 Å. The

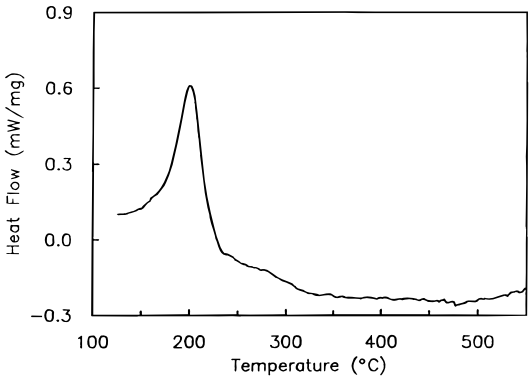

Figure 2. Representative differential scanning calorimetry data for selenium-rich molybdenum−selenium reactants (sample A-3) with the exotherm at 200 °C.

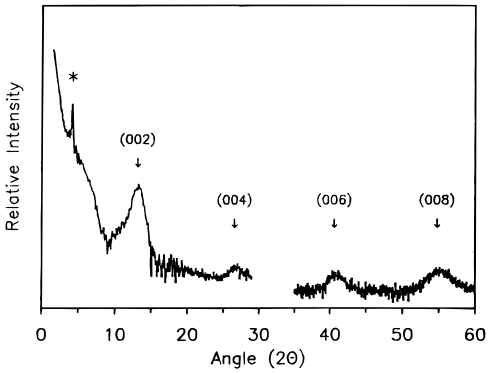

Figure 3. Diffraction data collected after annealing sample A-4 to 300 °C. The diffraction peak at 4° (*) is a Bragg diffraction maximum from the layering of the sample. The diffraction maxima labeled with indices are (00l) peaks of $MoSe_2$ (drysdallite-2H). The diffraction peaks from the silicon substrate have been removed from 29 to 35°.

compositions, determined via microprobe analysis, are also in agreement with the intended layer thicknesses, since a linear relationship exists between the ratio of the intended layer thicknesses and the measured composition.

The results of the calorimetry and diffraction studies showed that the samples could be grouped into four classes depending on their composition and the structure observed after annealing to 550 °C. The most selenium-rich class of samples, containing more than 45 atom % selenium (the A group of samples), all contained crystalline $MoSe_2$ after annealing to 550 °C. Two different reaction pathways were observed for these samples. The reaction pathway depended on both the composition and repeat layer thickness of the sample. In general, samples with a repeat thickness greater than 20 Å showed evidence for heterogeneous nucleation of $MoSe_2$ at the reacting interfaces. The DSC of these samples showed a low-temperature exotherm near 200 °C, as shown in Figure 2. Diffraction data (shown in Figure 3) clearly show the formation of crystalline $MoSe_2$ concurrent with low-angle diffraction maxima, indicating that the sample remains elementally modulated. The size of the low-temperature exotherm and the crystallinity of the resulting $MoSe_2$ depended on the composition of the sample. Samples with stoichiometric compositions had much sharper $MoSe_2$ diffraction maxima after annealing to 550 °C, indicating larger crystallite size, than samples which were more molybdenum rich. Samples with smaller repeat thicknesses had no readily apparent low-temperature exotherm in the DSC. Instead, an exotherm was observed at higher temperatures, from 350 to 500 °C. The resulting product, $MoSe_2$, has significantly larger crystallites than samples with nearly identical compositions but larger initial repeat thicknesses. This is consistent with an earlier

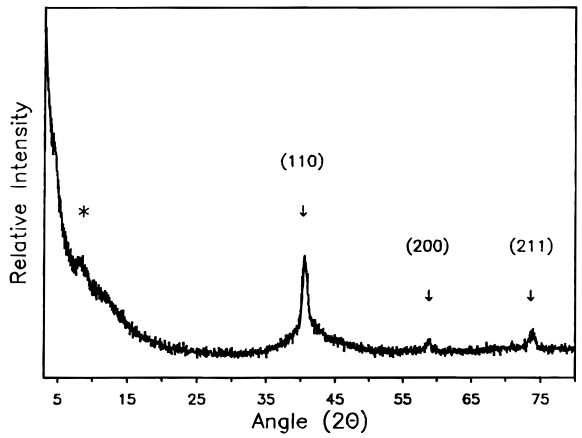

Figure 4. Diffraction data collected after annealing sample B-2 to 550 °C. The diffraction peak at 8° (*) is a Bragg diffraction maximum from the layering of the sample. The diffraction maxima labeled with indices are consistent with very small crystallites of molybdenum.

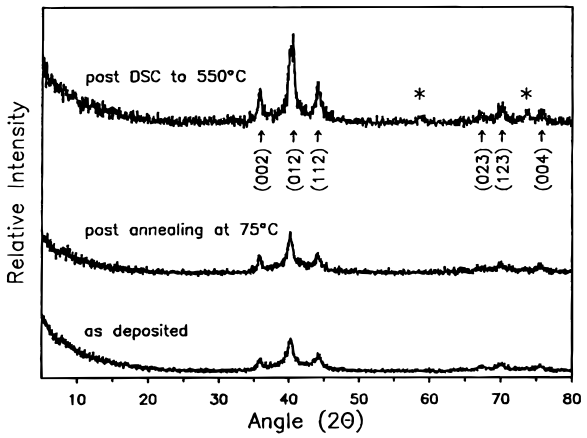

Figure 5. Diffraction data collected as a function of annealing time and temperature on sample C-5. The diffraction peak at 7° is a Bragg diffraction maximum from the layering of the sample. The diffraction peaks at 59 and 73° (*) are from crystalline molybdenum. The diffraction maxima labeled with indices are from the new compound Mo_3Se, which is already present in the as-deposited sample.

study that examined the formation of $MoSe_2$ as a function of repeat thickness at a constant composition and suggests that nucleation does not occur at the interfaces during the mixing of the layers.[3]

The second class of samples (group B) were more molybdenum rich (between 43 and 35% selenium). In these samples, no exotherms are observed in the calorimetry data. X-ray diffraction data collected after annealing at 550 °C showed that very small crystallites of molybdenum had formed. As shown in Figure 4, the diffraction pattern after ramping sample B-2 to 550 °C in the DSC still show evidence for elemental modulation. Annealing these samples to 1200 °C resulted in the formation of a mixture of molybdenum metal and Mo_3Se_4, as predicted from the accepted phase diagram.

In samples with a higher concentration of molybdenum, a third class of reactivity was observed. In samples C-1−C-5, a weak exotherm near 210 °C was observed in the DSC. Diffraction data collected as a function of annealing showed the heterogeneous nucleation of a new compound (Figure 5). The diffraction maxima for this new compound became sharper and more intense as the composition approached Mo_3Se. Three additional samples were prepared at this composition with variations in the layer thicknesses (samples C-6−C-8). These samples also showed the formation of this new compound on deposition. The structure of this new compound was deduced

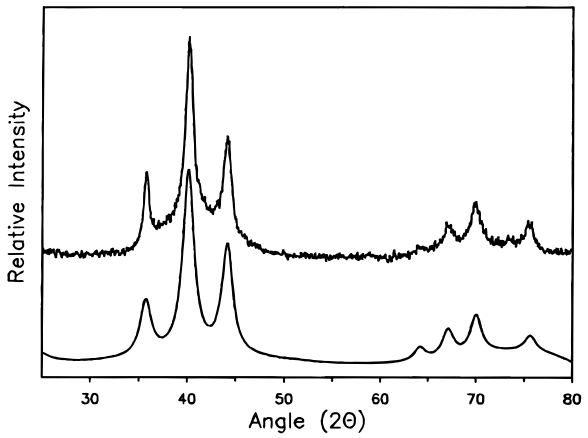

Figure 6. Comparison of the calculated and observed diffraction pattern of the new compound Mo_3Se.

from the diffraction pattern. Since the diffraction pattern contained only a few lines and rocking curve studies indicated no preferred orientation, the unit cell must be small and have high symmetry. These peaks could be indexed with a cubic unit cell, $a = 5.03$ Å. Comparisons with known structures containing a 3:1 composition ratio (for example, Mo_3Si) suggested that the new compound has the A-15 structure. The structure was refined in space group O_h^3-$Pm\bar{3}n$ using Reitveld refinement (DBWS-9006PC).[14] The atoms in Mo_3Se reside on special position sites, with 2 Mo in Wyckoff positions a [(0, 0, 0) and ($^1/_2$, $^1/_2$, $^1/_2$)] and 6 Se in Wyckoff positions c [($^1/_4$, 0, $^1/_2$), ($^1/_2$, $^1/_4$, 0), (0, $^1/_2$, $^1/_4$), ($^3/_4$, 0, $^1/_2$), ($^1/_2$, $^3/_4$, 0), and (0, ($^1/_2$, $^3/_4$)].[15] Refining the unit cell size and line widths resulted in a good agreement between the calculated pattern and the experimentally observed diffraction pattern as shown in Figure 6. The refined unit cell size of Mo_3Se (5.092 ± 0.001) is larger than that reported for Mo_3Si (4.890 ± 0.002). Allowing the occupancies to vary during the refinement did not lower the residual below the value of $R_{wp} = 9.1$ obtained by fixing the occupancies at 1. This is in part because the quality of the diffraction data precludes increasing the number of fitting parameters beyond those required to fit the background, line shapes, and unit cell size. The unit cell size was not found to vary as the molybdenum to selenium ratio was varied, suggesting that this new compound is stable only within a small composition range. Annealing a sample of this new compound at 1000 °C resulted in the formation of a mixture of Mo and Mo_6Se_8, as expected from the accepted phase diagram. The fourth class of samples, those more molybdenum rich than those which formed Mo_3Se, showed only the formation of crystalline molybdenum upon annealing.

Compounds with the A-15 structure are well-known as the compounds with the highest superconducting critical temperatures (T_c) until the discovery of the superconducting copper oxides. Mo_3Se has one more electron than Nb_3Sn ($T_c = 18$ K) and Nb_3Ge ($T_c = 23$ K) and is isoelectronic with Nb_3Al which has a T_c of 18 K. To determine if Mo_3Se superconducts, we measured the magnetic susceptibility as a function of temperature. The observed susceptibility was small (-20×10^{-6} emu/mol uncorrected for core diamagnetism), diamagnetic, and temperature independent, indicating that the Pauli paramagnetism of the conduction electrons in Mo_3Se was not sufficiently large to overcome the diamagnetism from the atomic cores. The sample undergoes a sharp diamagnetic transition at 2.2 K,

(14) Sakthivel, A.; Young, R. A. Thesis, School of Physics, Georgia Institute of Technology, Atlanta, GA 30332.
(15) Templeton, D. H.; Dauben, C. H. *Acta Crystallogr.* **1950**, *3*, 261−262.

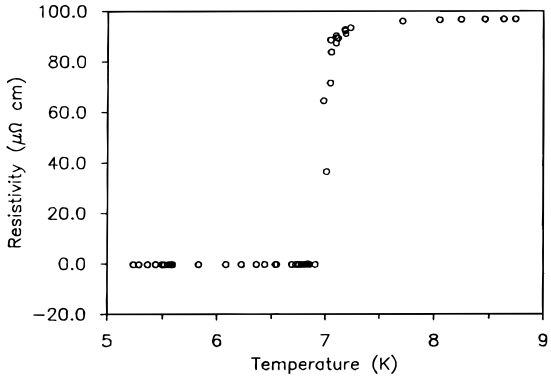

Figure 7. Resistivity as a function of temperature for Mo_3Se (sample C-6). The abrupt decrease in conductivity at 7 K signals the superconducting transition.

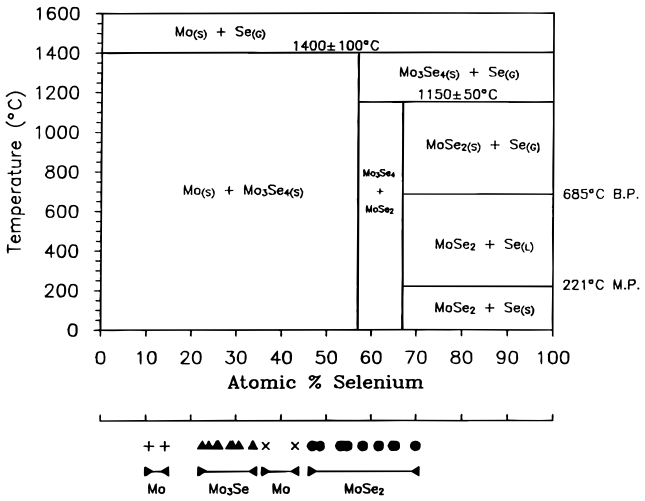

Figure 8. Comparison of the thermodynamic phase diagram with the observed nucleation behavior of the films studied.

indicative of a superconducting transition. The resistivity as a function of temperature is shown in Figure 7 for a sample made in a different deposition than used in the susceptibility study. The data were collected on a film deposited upon a silicon wafer and indicate that Mo_3Se is metallic and undergoes a sharp drop in resistance at approximately 7 K. The difference between the behavior of this film and the powder used in the susceptibility study presumably results from a small difference in stoichiometry.

Figure 8 summarizes the behavior of the samples studied, contrasting the equilibrium behavior given by the thermodynamic phase diagram with a kinetic "phase diagram" based on the observed nucleation behavior. There are two distinct differences between the accepted equilibrium behavior and kinetic phase formation at reacting interfaces—the formation of a new compound Mo_3Se and the inability to form the equilibrium compound Mo_6Se_8.

The new compound, Mo_3Se, appears to have a limited composition range, since its lattice parameters remain constant with variable composition of the reactant. It only forms around a 3:1 ratio of Mo:Se. Mo_3Se was found to have the A-15 structure and was found to be kinetically stable to at least 550 °C. We have insufficient data to determine whether Mo_3Se can exist in equilibrium with Mo or Mo_6Se_8 below its decomposition temperature. It peritectically decomposes between 600 and 1000 °C. There are at least two possibilities that can explain why Mo_3Se has not been observed before, given its relative stability. If Mo_3Se is thermodynamically more stable than a mixture of molybdenum and Mo_6Se_8 at low temperatures, kinetics have prevented its discovery. Phase diagrams have traditionally been explored by examining the transformation between products as temperature is decreased. If the kinetics of the reaction between solid phases is slow, for example between Mo and Mo_6Se_8, it will be exceedingly difficult to find evidence for compounds which are only stable at low temperatures, especially if they peritectically decompose. This is especially true if there is no low-temperature eutectic close to the composition of the low-temperature compound.[2] If Mo_3Se is thermodynamically less stable than a mixture of molybdenum and Mo_6Se_8 at all temperatures, its discovery was prevented by the inability to control reaction intermediates in solid state synthesis. In this case, one needs to prevent the formation of other thermodynamically more stable binary compounds to observe the formation of this kinetic product. In either case, the multilayer precursor method is ideal for determining if low-temperature compounds exist, since it avoids competing compounds as reaction intermediates and eliminates diffusion as the rate-limiting step in phase formation.

The second difference between the accepted equilibrium behavior and the observed kinetic phase formation was the inability to form Mo_6Se_8. We believe that Mo_6Se_8 is not formed because it may be more difficult to nucleate than either $MoSe_2$ or Mo_3Se. The relatively lower nucleation energies of $MoSe_2$ and Mo_3Se relative to Mo_6Se_8 may simply be a function of the complexity of their structures. Both $MoSe_2$ and Mo_3Se are relatively simple structures which can be thought of as consisting of simple building blocks that share either edges or faces.[16] In $MoSe_2$, molybdenum is surrounded by a trigonal prism of selenium. These trigonal prisms share square faces to form two-dimensional layers. In Mo_3Se, molybdenum is surrounded by a tetrahedron of selenium atoms. The tetrahedra share edges to form the cubic A-15 structure. One would expect both these local molybdenum coordinations to exist in relatively high concentrations in the amorphous intermediate. The Mo_6Se_8 structure is more complicated, consisting of an octahedron of molybdenums with each triangular face capped with a selenium atom. These cluster units then pack to avoid Se−Se repulsions and form weak Mo−Se bonds between cluster units. To nucleate this structure from the amorphous intermediate, one presumably has to form the molybdenum octahedra and then either aggregate the preformed octahedra or have additional atoms attach to the central octahedral cluster. To form this octahedron of molybdenum atoms, one must exclude selenium from this volume. The Mo_6Se_8 structure involves arranging considerably more atoms than either the Mo_3Se or $MoSe_2$ structures, and the "building blocks" of this structure probably differ considerably from the local coordination preferences of the molybdenum in the amorphous intermediate.

The inability to nucleate Mo_6Se_8 highlights one of the remaining challenges in the development of modulated elemental reactants as a synthetic method. If the activation energy for interdiffusion of the initially layered reactant to the homogeneous intermediate is higher than the energy to heterogeneously nucleate one of the other binary products at the reacting interfaces, Mo_6Se_8 will not be the first compound formed. If the layers interdiffuse to form a homogeneous intermediate, the inability to nucleate Mo_6Se_8 has to do with its relative nucleation energy with respect to the other binary compounds. One needs to develop synthetic parameters and strategies to modify and control relative nucleation energies to permit selective nucleation of targeted compounds.

(16) Wells, A. F. *Structural Inorganic Chemistry*, 5th ed.; Clarendon Press: Oxford, U.K., 1984; pp 1−1382.

Conclusions

Multilayer elemental reactants have been used to examine the kinetics of phase formation in the molybdenum−selenium system. We observed facile, low-temperature nucleation and growth of $MoSe_2$ and a new molybdenum selenide, Mo_3Se, which is stable below 550 °C. In contrast, we were unable to nucleate the other previously known molybdenum selenide, Mo_6Se_8, at low temperatures. The new molybdenum selenide, Mo_3Se, was found to superconduct. The T_c was measured to be 2.2 K from susceptibility data, while a second sample had a T_c of 7 K determined from conductivity measurements.

Acknowledgment. The support of the National Science Foundation (Grants DMR-9308854 and DMR-9510562) is gratefully acknowledged.

IC9708125